

Automated assessment of cardiac morphological variation in Atlantic salmon (*Salmo salar* L.)

Lisa-Victoria Bernhardt^{a,*}, Andreas Hafver^{a,1}, Nafiha Usman^a, Edward Yi Liu^a, Jørgen Andreas Åm Vatn^a, André Ødegårdstuen^b, Heidi S. Mortensen^c, Ida Beitnes Johansen^d

^a DNV AS, P.O. Box 300, 1322, Høvik, Norway

^b Adigo Mekatronikk, P.O. Box, 1405, Langhus, Norway

^c Firum P/F · Við Áir 11, FO-430, Hvalvík, Faroe Islands

^d NMBU, The Norwegian University of Life Sciences, P.O. Box, 1433, Ås, Norway

ARTICLE INFO

Keywords:

Computer vision
Cardiac morphology
Atlantic salmon
Aquaculture
Morphometrics

ABSTRACT

Deviating heart shapes and poor cardiac health is a recurring concern in farmed Atlantic salmon. Morphometric analysis has so far improved our understanding of salmonid cardiac morphology, but assessment of morphological cardiac variation is usually performed manually through measurements of lengths, ratios, and angles. Manual assessment of heart shape is tedious, time-consuming, and not very standardized. It also requires training and alignment of personnel to achieve reliable results. Considering these challenges, we aimed to automate this process using a deep learning model for computer vision to measure the morphological variations of the heart. Here we developed an algorithm for a diagnostic tool to detect variation in cardiac morphology in farmed Atlantic salmon, which we believe can assess cardiac morphological variation in a more objective, reproducible, and reliable manner compared to the manual process. The knowledge derived from this study may represent a crucial step in comprehending and eventually reducing cardiac abnormalities in farmed salmonids, which is essential for improving fish health and welfare and ensuring aquaculture's sustainable growth.

1. Introduction

Farming of Atlantic salmon (*Salmo salar* L.) is expanding globally, and marine aquaculture is expected to intensify even further in the future. A serious challenge to future growth and development of the aquaculture industry is intolerably high mortality of fish. This mortality is not only a rough indicator of poor welfare (Grefsrud et al., 2024), but it also poses a serious obstacle to the sustainability, ethics, and economy of the Nordic aquaculture industry. In recent years, the annual mortality rate of farmed Atlantic salmon in Norway has been high but stable during the sea stage, with a mortality of 16.7% (calculated as the cumulative mean mortality risk) for all completed production cycles in 2023 (Sommerset et al., 2024). Similarly, a mortality rate of 10.2% during the sea stage was observed in the Faroe Islands in 2023 (calculated as the general mortality rate for all completed production cycles) (Rúni Dam, Avrik sp./f, unpublished data), which is a decrease from previous years. Although the causes underlying this massive mortality are poorly charted, stressful procedures including delousing, handling,

and transport are factors associated with baseline mortality in Norwegian Atlantic salmon farming (Oliveira et al., 2021). Furthermore, there is an increasing body of evidence suggesting that a large fraction of farmed fish die from heart-related issues associated with deviating cardiac morphology and/or disease after exposure to stressful routine field treatments (Engdal et al., 2024; Frisk et al., 2020; Poppe et al., 2003).

Already two decades ago, Poppe et al. (2003) observed that farmed Norwegian Atlantic salmon have more heart shape deformities compared to their wild counterparts, which has also been confirmed by a more recent study (Engdal et al., 2024). More specifically, the ventricles of farmed salmon hearts tend to be rounded and asymmetrical with a misaligned outflow tracts (i.e. bulbus arteriosus, hereby referred to as bulbus) which links to the ventral aorta to supply arterial blood to the gills. Knowledge about the causes behind these cardiac morphological abnormalities are beginning to emerge and are likely multifactorial. For instance, it has been suggested that heart shape can be influenced by both environmental factors and rearing intensity early in life (Engdal et al., 2024; Frisk et al., 2020). The functional consequences of deviating

* Corresponding author: DNV AS, P.O. Box 300, Høvik 1322, Norway.

E-mail address: lisa.victoria.bernhardt@dnv.com (L.-V. Bernhardt).

¹ These authors contributed equally

heart shape are also not fully understood but have been directly linked to impaired cardiac and physical performance (Claireaux et al., 2005) as well as mortality following stressful aquaculture operations (Engdal et al., 2024; Frisk et al., 2020).

Engdal et al. (2024) recently published an easy qualitative approach involving a standardized protocol for recording and monitoring heart shape of Norwegian Atlantic salmon. They based it on an extensive library of photographs of hearts from farmed Atlantic salmon collected in connection with fish health surveillance and project samplings. From this they confirmed differences between farmed and wild Atlantic salmon, consistent with previous research (Poppe et al., 2003). Moreover, they were able to identify 38 common morphological traits in hearts from Norwegian farmed Atlantic salmon of which certain traits were associated with mortality, indicating the potential of heart shape as a risk assessment tool (Engdal et al., 2024).

Currently, cardiac morphological assessment typically includes manual inspection and/or measurements to investigate heart shape or other ventricular characteristics (e.g. bulbus positioning and fat deposits). Quantitative approaches involve measurement of cardiac lengths, angles, and ratios to reveal several cardiac morphological traits and are fairly objective. The recently published qualitative method involves a macroscopical inspection of the heart and is a more subjective approach. The quantitative approach is suitable for describing morphological development over time and comparing distinctly contrasting groups (e.g., wild versus farmed Atlantic salmon), making it more reproducible, but less representative, than the qualitative assessment. However, although the qualitative approach can reveal more extreme traits and other traits that haven't been found quantitatively, it is still necessary to have some user training to achieve reliable and representative results when performing the assessment qualitatively. Hence, it has been recommended by Engdal et al. (2024) to combine the qualitative and the quantitative approaches to gather sufficient information and uncover the true variation in heart shape deformities of the Atlantic salmon.

The current assessment of Atlantic salmon hearts is performed through manually segmenting and measuring shapes and angles of the

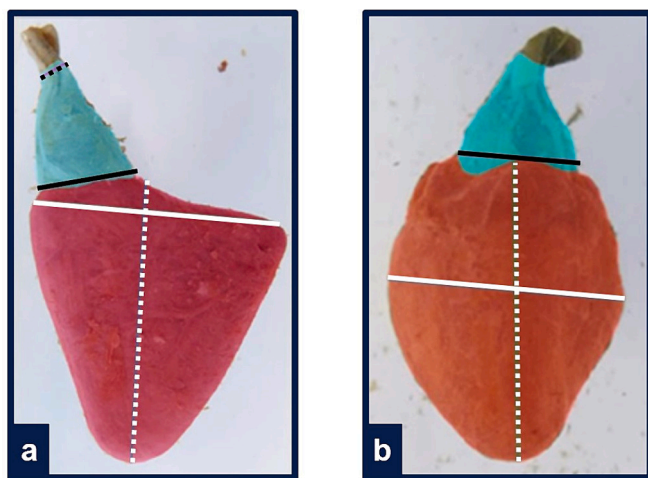


Fig. 1. Examples of annotated heart images from Atlantic salmon, performed by human domain experts using Labelbox. Two projections were used to train and validate the computer vision models. In a) the left lateral projection the white solid line represents ventricular width, the white dotted line the ventricular height, black solid line the bulbus width on its widest by the bulboventricular junction, and black dotted line the bulbus on its narrowest. In b) the ventrodorsal) projection, the white solid line represents the ventricular width, white dotted line the ventricular height, and black solid line the bulbus width on its widest by the bulboventricular junction. Note that the fatty area between bulbus and the ventricle are both omitted, as well as the ventral aorta above bulbus.

heart, which is a tedious, time-consuming, and not standardized process. Site or farm specific scoring systems are often used, performed by producers or fish health personnel and training and alignment is required to ensure consistent measurements of the cardiac morphology (Engdal et al., 2024). Moreover, there are challenges with existing measurement methods that remain, including few landmarks for morphometrical analysis, insufficient user training and thereby disagreement between personnel to make reproducible, reliable, and more objective measurements. To solve these challenges and accommodate future expansion of marine aquaculture, we believe that this sector must continue to place a high priority on technical innovation to achieve sustainability and improved fish health and welfare. Currently, to our knowledge, there is no approach to measure heart shape deformities automatically. This could be achieved by using machine learning models for computer vision that could automate the quantitative approach. Machine learning and computer vision have already found various applications in aquaculture, for example in fish biomass estimation, recognition and classification of fish, behavioral analysis, and water quality prediction (Liu et al., 2023; Zhao et al., 2021).

The main aim of this study was to develop an algorithm for a diagnostic tool, to automate measurements and investigate variation in cardiac morphology in farmed Atlantic salmon. Measurement and understanding of cardiac morphometry may be important for breeding programmes, where selection for commercial traits (e.g., growth, and disease resistance) may inadvertently impact cardiac health (Taylor et al., 2015). Thus, the knowledge derived from this study could assist future endeavors to identify operational practices and environmental factors that underlie the development of heart shape variations and health. Digitalization could enhance fish health management and hence enable sustainable growth in aquaculture through improved fish welfare, mitigation of production losses, and reduced environmental footprint.

2. Materials and methods

2.1. Sampling of hearts

Hearts were collected from farmed Atlantic salmon during the seawater phase in connection with fish health surveillance and project samplings from different geographical locations in Norway and the Faroe Islands. We used a total of $n = 3742$ hearts ($n = 2969$ from Norway; $n = 773$ from the Faroe Islands) of farmed Atlantic salmon and these were photographed in three different projections according to the anatomical nomenclature described by Engdal et al. (2024); ventrodorsal (VD), left lateral (LL) and right lateral (RL).

The heart images from the farmed Norwegian Atlantic salmon were provided by Aqua Kompetanse AS, AquaGen, Ellingsen Seafood, and SalMar. The heart images from the farmed Faroese Atlantic salmon were provided by three different aquaculture companies (i.e. Bakkafrost, Hiddenfjord and Mowi Faroe Islands). In addition to this, we used $n = 122$ images of wild Atlantic salmon hearts received from the Norwegian University of Life Sciences (NMBU, Ås, Norway). These had been sampled from the southern parts of Norway in August 2021. All heart images used in this study were received and stored securely in DNV's Veracity data platform.

Note that we only know the age of the fish and how it died for a small subset of heart images. For one of these subsets the hearts were labelled as either Dead ($n = 61$ from Norway; $n = 20$ from the Faroe Islands) or Survivor ($n = 40$ from Norway; $n = 40$ from the Faroe Islands). Some of the Norwegian hearts were labelled as Smolt ($n = 247$) or Adult ($n = 296$). For all these groups we used images from three projections (VD, LL and RL) for the analysis.

2.2. Imaging of hearts

After euthanization, intact hearts (bulbus, ventricle and atrium) from

Table 1

An annotation guideline over the quantitative measurements of heart images from Atlantic salmon in (a) left lateral and (b) ventrodorsal projections, respectively. The description is based on the anatomical nomenclature as given by Engdal et al. (2024).

| (a) Left lateral measurements | Description |
|-------------------------------|---|
| “Top” bulbus width | Bulbus on its narrowest, i.e. the line perpendicular to bulbus axis and parallel to bulbus top cut-off (black dotted line, Fig. 1a). Note: This was not measured with the image segmentation model described in section 2.4. |
| “Bottom” bulbus width | Bulbus width on its widest by the bulboventricular junction (black solid line, Fig. 1a) |
| Ventricular width | The ventricle on its widest. For a normal heart shape, it would be the length between the ventral ventricular apex (by the ventriculobulbar groove), and the left dorsal ventricular apex (white solid line, Fig. 1a). |
| Ventricular height | The ventricle on its longest, i.e., the length between the caudal ventricular apex and the ventriculobulbar groove (white dotted line, Fig. 1a) |
| (b) Ventrodorsal measurements | Description |
| “Bottom” bulbus width | Bulbus width on its widest by the bulboventricular junction (black solid line, Fig. 1b) |
| Ventricular width | The ventricle on its widest. For a normal heart shape, it would be the length between the right dorsal ventricular apex and the left dorsal ventricular apex (white solid line, Fig. 1b) |
| Ventricular height | The length from the midpoint of the line for the “bottom” bulbus width (typically by the ventriculobulbar groove) to the caudal ventricular apex (white dotted line, Fig. 1b). |

Atlantic salmon were dissected out and placed in PBS containing 50 mM KCl to stop the heart from beating. Following this procedure, hearts from Norway were fixed in 70% ethanol or 4% buffered formaldehyde and stored at 4 °C, while hearts from the Faroe Islands were fixed in 4% formalin and stored at room temperature. The atrium was carefully removed either before or after fixation at the atrioventricular junction (based on the anatomical nomenclature as given by Engdal et al., 2024). Thereafter, hearts from Norway were transported to the NMBU where they were submerged in water and then mounted under water on a pushpin glued to the bottom of a custom-made transparent plastic box placed on top of a light plate (Slimlite LED, 32 × 22.8 cm, Kaiser, Buchen, Germany). The Faroese hearts were transported to Firum (Hvalvík, Faroe Islands) where they were submerged into a custom-made transparent plastic box filled with freshwater and mounted on a pushpin glued to the bottom of the box under water. Canon Powershot SX540 HS (Canon Inc., Tokyo, Japan) camera was used to photograph the Norwegian heart from above in three different projections: VD, LL and RL. For the Faroese hearts, the camera was placed in the middle of a ring light to photograph them from the same three different projections as for the Norwegian hearts.

2.3. Annotation of heart images

A total of 1017 images of Atlantic salmon hearts were annotated by domain experts with Labelbox (<https://labelbox.com>) and they were all used to train and validate the computer vision models (Fig. 1). Only VD projections ($n = 460$ images) and LL projections ($n = 557$ images) were annotated in accordance with the guidelines provided in Table 1. This guideline was developed in an iterative manner as a collaboration between domain experts and computer vision engineers. The annotated heart images were split into training and validation datasets (90% and 10%, respectively). The images with corresponding annotations were used to train and validate an image segmentation model to detect bulbus and the ventricle of the Atlantic salmon heart.

2.4. Development of model

At the outset of this study, we trained two kinds of machine learning models. Firstly, we trained the image segmentation model to locate the ventricle and bulbus of the Atlantic salmon hearts. Secondly, we trained the object detection models to detect the location of landmark points in VD and LL projections (i.e., the points annotated by humans, see section 2.3). However, in this study, we only used the image segmentation model.

Although the object detection models worked well to detect the landmark points in the training images, we observed early on that it was sensitive to changes in how the images were taken (e.g., light conditions, background, bubbles) and required retraining when images were received from new providers. This may have been possible to solve with more training data and augmentation of images. However, we were able to circumvent this problem. We found that the same landmark points could be reliably identified from the segmented heart images by using an algorithm instead of relying on machine learning. Thus, only the image segmentation model was needed in this step, and this model was also more robust to the imaging conditions. This image segmentation model could be used to detect the ventricle and bulbus in heart images taken from the LL, VD and RL projections.

Hence, the morphometric method developed in this study has the following workflow, as described here and in more detail in the sub-sections below:

1. The images were segmented to locate the ventricle and bulbus of the heart.
2. The segmented heart images were processed to extract physically meaningful contours of the ventricle and bulbus.
3. Landmark points were computed from the heart contours.
4. A dimension reduction technique (Uniform Manifold Approximation and projection, UMAP) was used to identify the key characteristics of the cardiac morphology in Atlantic salmon, based on all the heart images.

The performance relating to point 1 and 2 were measured using Intersection over Union (IoU) of human versus the model segmentations. For point 3, comparison between human and computer measurements were made by computing ratio of measured ventricular height, ventricular width and bulbus width.

2.4.1. Segmenting the heart images

A Feature Pyramid Net (FPN) model (He et al., 2015) with `se_resnetxt50_32x4d` encoder (Xie et al., 2016) pretrained on the ImageNet dataset (Deng et al., 2009) was used to segment bulbus and the ventricle of the Atlantic salmon heart images. A total of $n = 134$ heart images in two different projections (LL and VD) were used to train the segmentation model, and the following augmentations were used to increase the diversity and size of the training dataset: Random-Flip, Shift-Scale-Rotate, Contrast Limited Adaptive Histogram Equalization (CLAHE), Random-Brightness-Contrast, Random-Gamma, Hue-Saturation-Value, Sharpen, Blur, MotionBlur. For the training and validation, heart images were resized to 416×544 . An example of an input heart image is shown in Fig. 2a, and an example of a segmentation model output is shown in Fig. 2b.

2.4.2. Processing the segmented heart images to extract contours

For each heart image, the segmentation model outputs two arrays of the same dimension as the downscaled input image. The first output array contains values between 0 and 1, indicating the probability that the corresponding image pixel belongs to bulbus. Similarly, the second array indicates the probability that pixels belong to the ventricle. An example of the bulbus and ventricle extracted contours have been shown in Fig. 2c.

To extract the contours of the ventricle and bulbus, we applied the

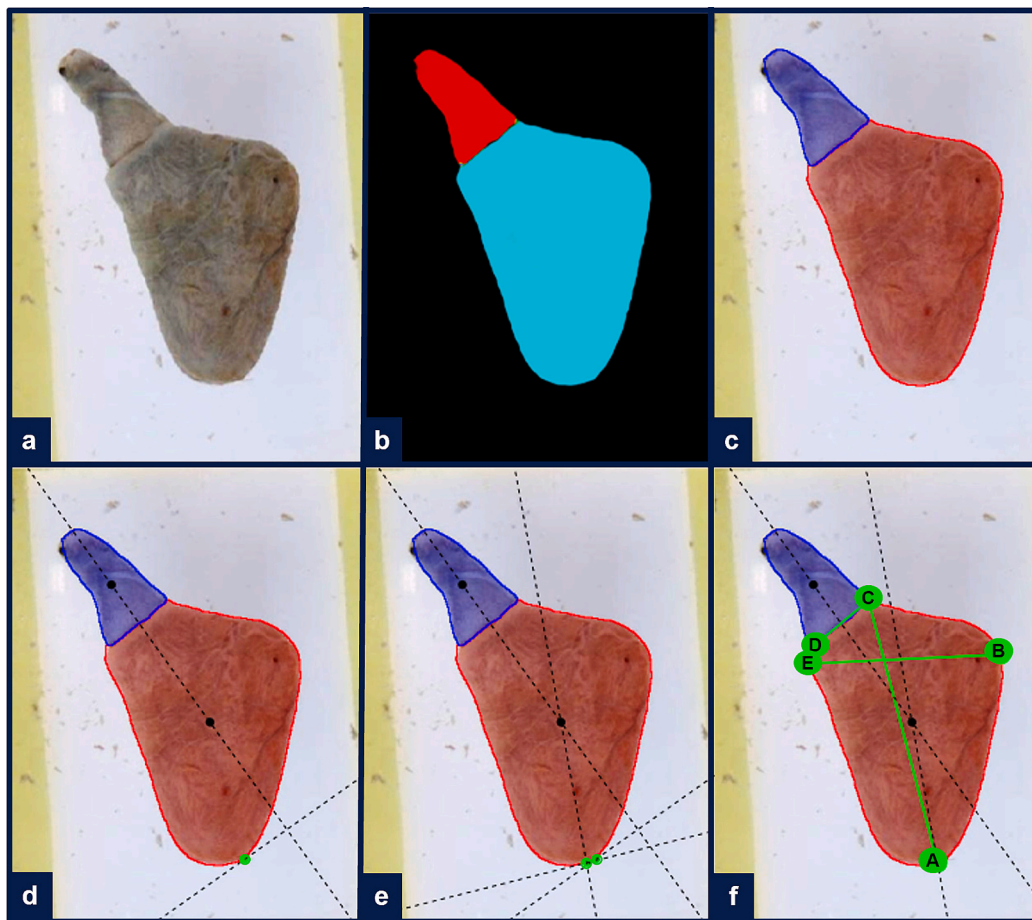


Fig. 2. The procedure to locate the algorithmic landmark points on a heart image from Atlantic salmon (here visualized in left lateral projection) (a-f). The first step involves (a) the input image of the heart, followed by (b) the raw output of the segmentation model, showing the probability of the ventricle (cyan) and the bulbus (red) (c) processing of the segmented heart image from b generating the extracted contours of the ventricle (red) and bulbus (blue), (d) identification of the centroids of the ventricle and bulbus (black points) and computing the first estimate of the lower ventricle apex point (green point) as the point on the ventricle that is furthest away from the bulbus along the line joining the centroids, (e) updating the lower ventricle apex estimate by repeating the procedure from d) along the line passing through the initial estimate of the lower apex point and the ventricle centroid. Finally, in (f) the point identified in e) is denoted by A and used as a landmark point for the caudal ventricular apex. We use the line through point A and the ventricle centroid to define the heart orientation, and define the left dorsal ventricular apex point B and the ventral ventricular apex point E (by the ventriculobulbar groove) as the points on the ventricle contour that are furthest away from this line. The points C and D are defined as the “corners” of the ventriculobulbar junction. (For interpretation of the references to colour in this figure legend, the reader is referred to the web version of this article.)

following steps:

1. We found the heart region by applying a threshold of 0.1 to the sum of bulbus and the ventricle arrays, resulting in a binary array/image. Any holes in the heart region of the binary array/image were then closed.
2. Bulbus was identified as the part of the heart region where the probability in the bulbus array exceeded the probability in the ventricle array.
3. We applied binary image erosion followed by binary image dilation to smooth bulbus and the ventricle regions. In cases where more than one connected region was identified for bulbus and the ventricle, only the largest one was kept.
4. The locations of the boundary pixels were used to extract the contour polygons of bulbus and the ventricle.

2.4.3. Measuring landmark points from contours

To measure the landmark points from the heart images, we first had to determine the orientation of the hearts. We did this by first drawing a line through the centroids of bulbus and the ventricle regions and finding the ventricle contour point furthest in the direction of the

ventricle (Fig. 2d). We then drew a new line through that point and the ventricle centroid and thereby found the furthest point on the ventricle contour again (Fig. 2e). This latter point is taken to be the caudal ventricular apex (point A), as shown in Fig. 2f. Defining the line through point A and the ventricle centroid as the center line, we identified the ventral ventricular apex and the left dorsal ventricular apex (points E and B, respectively). We also identified points C and D as the “corners” of the ventriculobulbar junction. Next, we measured the distances between the points (i.e., lengths of the line segments AB, AC, AD, AE, BC, CD, CE, and DE) as a way to quantify the cardiac morphology. Because we were only interested in the shape of the heart and not its actual size, lengths could be divided by the equivalent radius of the ventricle (i.e., $\sqrt{\text{ventricle area}/\pi}$) to remove any dependence on the pixel size of the heart in the images.

2.4.4. Heart shape quantification

For each heart image, we used the lengths of the line segments AB, AC, AD, AE, BC, CD, CE, and DE as geometrical features. Note that we did not measure angles between lines as additional features, because this information was already captured by the geometrical relationships between the line segments. These 8-dimensional geometrical features were

Table 2

Performance of the image segmentation model without post processing and with post processing using the intersection over union (IoU) and presented as mean \pm standard deviation.

| Approach | IoU, mean \pm standard deviation | | | |
|--|------------------------------------|-------------------------|-----------------------|-------------------------|
| | Ventricle | | Bulbus | |
| | Training (n = 915) | Validation (n = 102) | Training (n = 915) | Validation (n = 102) |
| Image segmentation model without post processing | 0.943 \pm 0.013 | 0.942 \pm 0.011 | 0.775 \pm 0.055 | 0.782 \pm 0.048 |
| Image segmentation model with post processing | 0.958 \pm 0.011 | 0.958 \pm 0.009 | 0.821 \pm 0.057 | 0.828 \pm 0.045 |

then reduced to two dimensions using the UMAP (Uniform Manifold Approximation and Projection) method (McInnes et al., 2018). UMAP is a popular dimension reduction technique that maps high-dimensional data to a lower-dimensional space by constructing a graph based on the pairwise distances between the data points in the high-dimensional input space. In this study, this dimension reduction technique was used as a tool to identify the distinct morphological traits in all the received Atlantic salmon heart images ($n = 10,145$ images taken in LL, VD and RL projections), from both Norway and the Faroe Islands.

2.5. Statistical analysis

The statistical analysis of the UMAP output was performed using Mathematica version 14.0 (Wolfram Research, Inc, 2024). We used the Mann Whitney test for pairwise comparison of different groups of heart images: Norway farmed ($n = 7842$ images), Faroe Islands farmed ($n =$

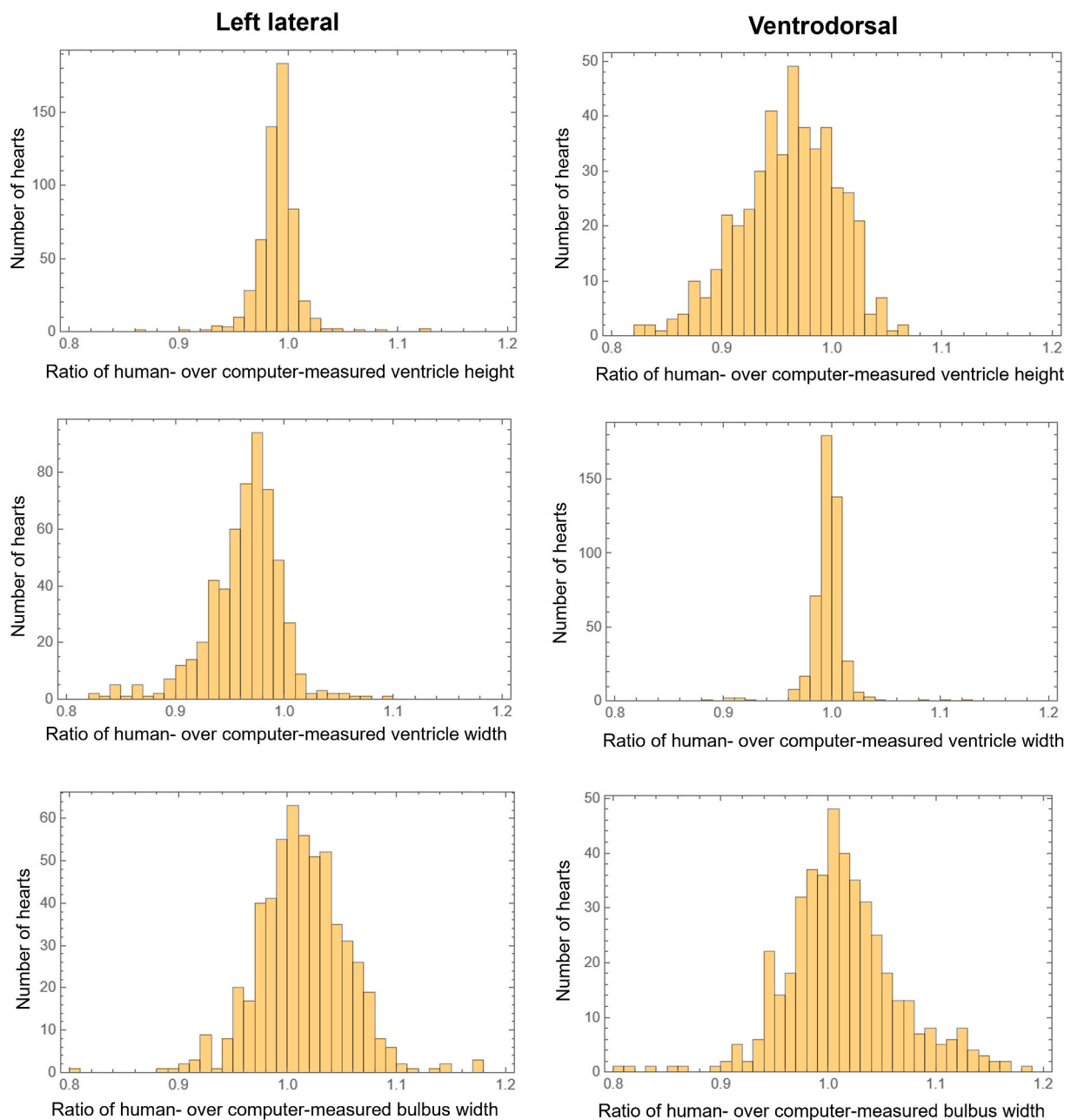


Fig. 3. Ratio of length measurements of ventricle height, ventricle width and bulbus width of hearts from Atlantic salmon, based on human- and computer-annotated heart images for the left lateral and ventrodorsal projections.

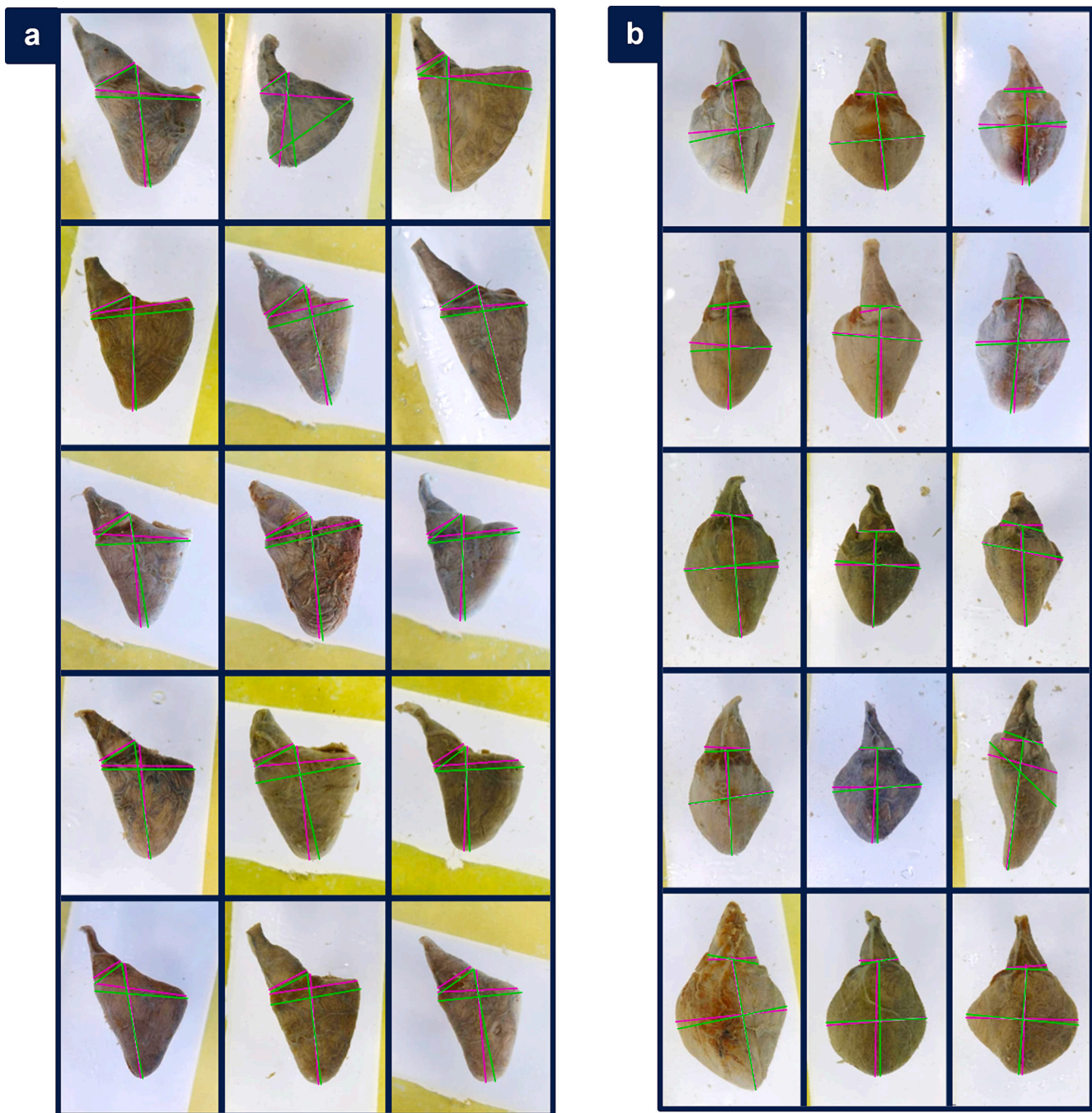


Fig. 4. Examples of measurements based on human annotation (pink) and computer annotation (green). Two different projections of the Atlantic salmon heart are visualized, including (a) left lateral, and (b) ventrodorsal. (For interpretation of the references to colour in this figure legend, the reader is referred to the web version of this article.)

2303 images), Smolt ($n = 247$ images), Adult ($n = 296$ images), Dead ($n = 243$ images), Survivor ($n = 240$ images) and Norway wild ($n = 122$ images). Note that we combine heart images from three projections (VD, LL, and RL) to have larger sample sizes and only compare the vertical UMAP output (UMAPy) which does not depend on the projections. The data was visualized as swarm plots with overlaid box plots using Python 3 and the Seaborn library (Waskom, 2021).

3. Results

3.1. Performance of the image segmentation model

To measure the performance of our image segmentation model and the post processing steps, we compared the IoU with the human annotations. The IoU is a real number in the range 0–1, and 1 means perfect overlap with the human annotation.

Table 2 shows the performance of the segmentation with and without post processing (described in section 2.4.2). We observed that the performance is consistently better for the segmentation of the ventricle compared to bulbus. We also observed that the results are very similar

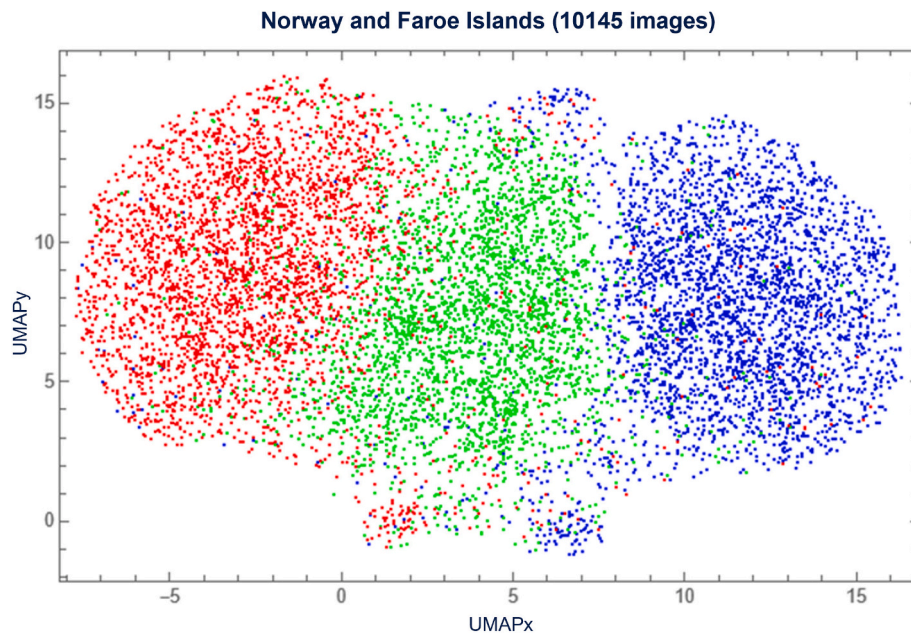


Fig. 5. shows the result of applying the UMAP dimension reduction (from 8 to 2 dimensions) on the measurements of $n = 10,145$ heart images ($n = 3742$ Atlantic salmon) from Norway and the Faroe Islands. The distribution of heart shapes from Norway and the Faroe Islands are shown in Fig. 6.

on the training data and validation data in all cases. However, with the post processing we observed that the IoU improves for both bulbus and ventricle segmentation on both the training- and validation datasets.

3.2. Automated heart measurement

For each heart image, we computed the landmark points A-E as shown in Fig. 2f. From these points we could calculate the ventricle height and width, as well as the bulbus width. Specifically, we took the line BE to be the ventricle width, and CD to be the bulbus width. For LL projections, we used the distance AC as the ventricle height, and for the VD projections we used the line between A and the midpoint of CD to measure the ventricle height.

To test the performance of the measurement algorithm, we compared the model output to human annotation (described in section 2.3) and computed the ratio of the lengths computed from human and computer annotated images (results shown in Fig. 3). Examples of the measurements based on human annotation and computer annotation, are shown in Fig. 4.

We observed that the human- and computer measurements mostly agree within 10% (as seen from the width of the histograms in Fig. 3, with much of the variation being within the 0.9–1.1 regions). Based on visual inspection of the histograms, it appears that the ventricle height measurement had the best agreement for the LL projections, and the ventricle width measurements had the best agreement for the VD projections (i.e. narrowest histograms in Fig. 3). Here we observed that the computer measures longer ventricle heights than humans on average, especially for the VD projections (i.e., the corresponding histogram in Fig. 3 is not centered at 1.0). Moreover, for the LL projections, the computer tended to measure longer ventricle widths than humans on average (i.e., the corresponding histogram in Fig. 3 is not centered at 1.0). The disagreement appears to be the largest for the bulbus width measurements (i.e., these have the widest histograms in Fig. 3).

3.3. Heart shape quantification

The first thing to note is from the horizontal direction (UMAPx, in Fig. 5) where the dimension reduction has been able to capture the heart projection as an important feature (seen from the separation of the

colours into three vertical bands corresponding to different projections, in Fig. 7). The reason for the variation and overlap between images from different projections is related to the placement as well as the actual variation of how symmetrical the hearts are within the same projection.

The second thing to note is that the vertical direction (UMAPy, in Fig. 5) is related to the height of the ventricle with the points located more towards the top section corresponding to hearts having elongated ventricles. In contrast, the points located more towards the bottom section in Fig. 5 have shorter ventricular length and therefore a rounder shape. In other words, the UMAP dimension reduction method suggests that the ventricular symmetry (UMAPx) and height:width ratio (UMAPy) are parameters that can help categorize cardiac morphological variation.

Lastly, the process flow for the automated morphometric analysis of the Atlantic salmon heart, starting with the collection and processing of data (i.e., heart images), followed by the development of model and heart shape quantification, has been illustrated in Fig. 8. Fig. 5: Uniform Manifold Approximation and Projection (UMAP) dimension reduction of the heart measurements. Each point is an image of a heart ($n = 10,145$ heart images in total, corresponding to $n = 7842$ images from Norway and $n = 2303$ images from the Faroe Islands). Grouping of the heart images is based on the heart shape, i.e., hearts that are similar to each other in shape are presented as points being closer to each other, while hearts that look different in shape are presented as points being farther apart. The three different colours indicate different heart projections, including right lateral (red points), ventrodorsal (green points), and left lateral (blue points).

3.4. Statistical comparisons between groups

Although comparing cardiac morphology across populations was not the main aim of the current study, comparisons were done to illustrate the potential applicability of the machine learning tool. Of note, the comparisons are based on a limited material and results should be interpreted with care. We can also not exclude the possibility that the use of different fixation methods might have affected the heart shapes slightly differently.

Hearts of farmed Atlantic salmon from Norway have a smaller UMAPy value than the hearts from farmed Atlantic salmon from the

Faroe Islands, indicating more elongated ventricular shapes (i.e. larger height:width ratio) of the Faroese hearts compared to the Norwegian hearts (Fig. S1). Similarly, the Norwegian farmed Atlantic salmon hearts seem to have a more rounded ventricular shapes (i.e. smaller UMAPy value), compared to the wild Atlantic salmon hearts, as shown by Fig. S1. Hearts from the dead fish (Dead in Fig. S1) had more rounded ventricular shapes than the survivors (Survivor in Fig. S1), and the adults (Adult in Fig. S1) had more rounded ventricular shape than the smolts (Smolt in Fig. S1). Results of statistical comparisons using the Mann Whitney test are shown in Tabel S1.

4. Discussion

In this study we have developed a method to perform measurements of heart from Atlantic salmon automatically. We have also shown that machine learning can be used to differentiate heart shapes, by projecting the heart measurements into a lower dimensional space. Below we discuss these results.

4.1. Heart measurement

The heart shapes of farmed Atlantic salmon typically deviate from that of their wild counterparts, which probably jeopardizes its overall health, welfare and therefore robustness (Claireaux et al., 2005; Poppe et al., 2003). Moreover, deviating traits have been found to be more prevalent in deceased fish after exposure to stressful routine field treatments (e.g. delousing) (Engdal et al., 2024). The most common diagnostic methods available to the aquaculture sector at the moment are PCR and histology, both of which are costly, time-consuming, and only provide a limited amount of information on organ function (Frisk et al., 2020). Heart shape analysis complements these other diagnostic methods in describing host risk factors. The value of automated heart shape analysis is the ability to process hearts from multiple individuals efficiently, which could for example have application for selective breeding.

The cardiac morphological assessment in salmonids can be performed with a qualitative method which is a subjective approach and/or with a quantitative method, which involves manually segmenting and measuring distances and angles and thus is an objective approach. However, one could argue that the quantitative measurements involve subjective judgment by humans who may not always agree on measurements of cardiac morphology. Regardless, these are manual, tedious, and time-consuming processes that require training and alignment of personnel to make consistent measurements (Engdal et al., 2024). To solve these challenges and accommodate future expansion of marine aquaculture, we believe that some of these processes can be achieved automatically by using machine learning models for computer vision and an algorithm. Hence, the main aim of this study was to combine domain biological knowledge with machine learning for a more objective, reliable, and reproducible cardiac morphometric analysis in Atlantic salmon, which may support our understanding of cardiac health impacts on fish welfare and enable a more sustainable aquaculture industry.

The field of morphometrics involves among other things methods to describe and compare shape variation within and among samples of organisms or structures (Rohlf and Marcus, 1993). Traditionally, it has been characterized by measurements of lengths and widths, and distances between certain landmarks of structures. Such samples may represent e.g., developmental stages, genetic and environmental effects (Rohlf and Marcus, 1993). However, geometric morphometrics (GM) including landmark- and outline-based GM methods have both been suggested to have several advantages over the “traditional” morphometric methodology (Lishchenko and Jones, 2021).

Previous research studies have assessed cardiac morphological variation with a quantitative approach which have been limited to a few measurements, including ratios and angles to quantify e.g. ventricular

roundness and the alignment of bulbus arteriosus (e.g. Engdal et al., 2024; Frisk et al., 2020; Poppe et al., 2003). Initially, dividing the ventricular height by ventricular width (i.e., the ventricular height:width ratio) and the alignment of bulbus arteriosus were selected as two simple, but yet adequate, quantitative measurements to describe the shape of the heart (Poppe et al., 2003). In that study, the ventricle height was defined as the length between ventricular apex and ventricular base whereas the ventricle width was defined as the length from the right dorsal ventricular apex to the left dorsal ventricular apex on VD surface. However, that ventricle height was modified by Frisk et al. (2020) to instead measure a line from the caudal ventricular apex to the ventriculobulbar groove on VD surface, and this measurement was also obtained by Engdal et al. (2024). Furthermore, the bulbus alignment on LL surface was measured by drawing a line from the caudal ventricular apex to the atriobulbar incision and a line following the midsection of the bulbus to the lines cross, generating an angle, according to Poppe et al. (2003).

In this study, we have selected landmark points on the heart, similarly to Engdal et al. (2024), but with minor alterations in order for them to be easily identifiable with an algorithm. Despite some differences between the human- and computer measurements in this study, the advantage of the latter is that they are based on a deterministic and reproducible algorithm, whereas the former relies on subjective judgment where some user training is required, which has also been stated by Engdal et al. (2024).

When looking at the heart images subjectively, the image segmentation model seems to perform well compared to the human segmentation of the Atlantic salmon hearts. In LL projections, the IoU is approximately 0.95, which is good, considering that even a human cannot be expected to perfectly trace the contour of the ventricle. The performance of our model on the bulbus segmentation is significantly lower than for the ventricle segmentation (i.e., IoU approximately 0.82 after post processing). This can be explained by the fact that it is somewhat ambiguous where the bulbus ends, particularly when there is a crown of epicardial fat, and even humans may not agree where to “cut” the top of the bulbus when they segment the hearts. We observed this when asking different domain experts to annotate the same image. However, the poorer performance on bulbus segmentation is not important for our measurement of the hearts, because the landmark points we ended up using only depend on the ventricle contour and the intersection of the ventricle and bulbus.

Unlike a human who can only measure a small number of landmark points, a computer can easily handle several. In this study we found that the human- and computer measurements agree well qualitatively in most cases. Even in cases where the disagreement is big, it is not clear if it is the former or the latter that provides the most reliable results. This could be because the exact locations of the ventricle's caudal-, left- and right- apex are ambiguous, but it could also be because the intersection of the ventricle and bulbus can sometimes be hard to locate precisely. In some cases, the computer measures long ventricle widths because the identified left- and right ventricle apex are misaligned, while a human may be inclined to measure the width of the ventricle more perpendicular to the ventricle's vertical axis.

It has been stated that environmental, and physical dependent plasticity can influence on the heart shape during the life cycle within one species (Poppe et al., 2003). In this context, a quantitative method's reproducibility becomes important. Previous research state that qualitative method is more suitable for differentiating distinctly contrasting groups (Engdal et al., 2024). In this study we found that the computer measurements facilitate better comparison between hearts sampled at different geographical locations, as it eliminates human biases. However, the computer measurements can be misleading from strongly deviating hearts, which could be explained by that the five landmark points (points A-E) were not sufficient to characterize extreme heart deviations, as discussed in section 4.2. Previous research has also stated that the qualitative method is more superior in detecting extreme

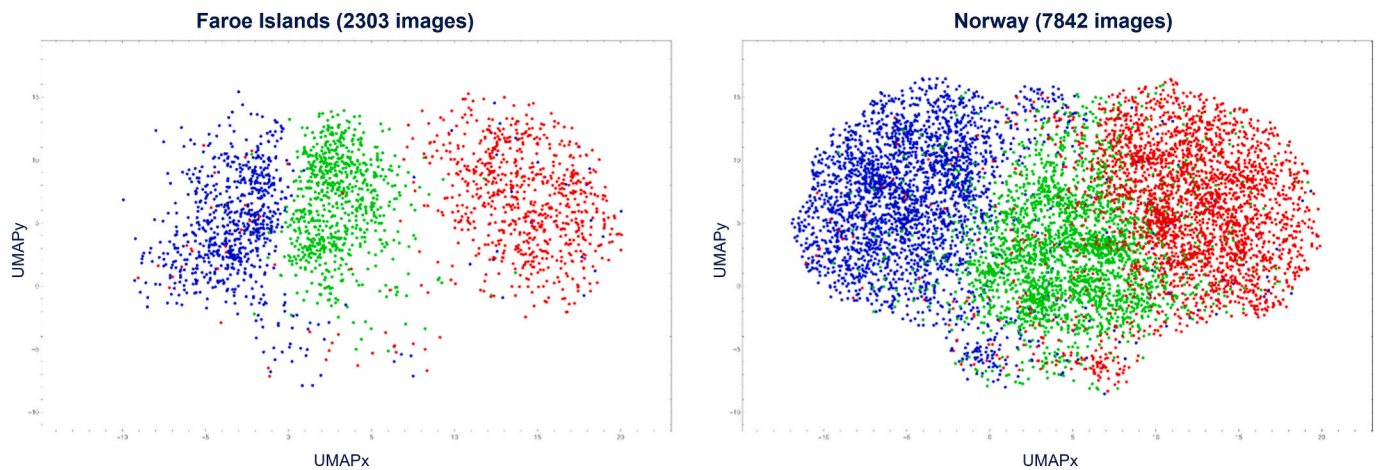


Fig. 6. The distribution of cardiac morphological variation in Atlantic salmon. Each point is an image of a heart where the points are grouped based on similarities in shape. The three different colours indicate different heart projections, including left lateral (blue points), ventrodorsal (green points), and right lateral (red points). (For interpretation of the references to colour in this figure legend, the reader is referred to the web version of this article.)

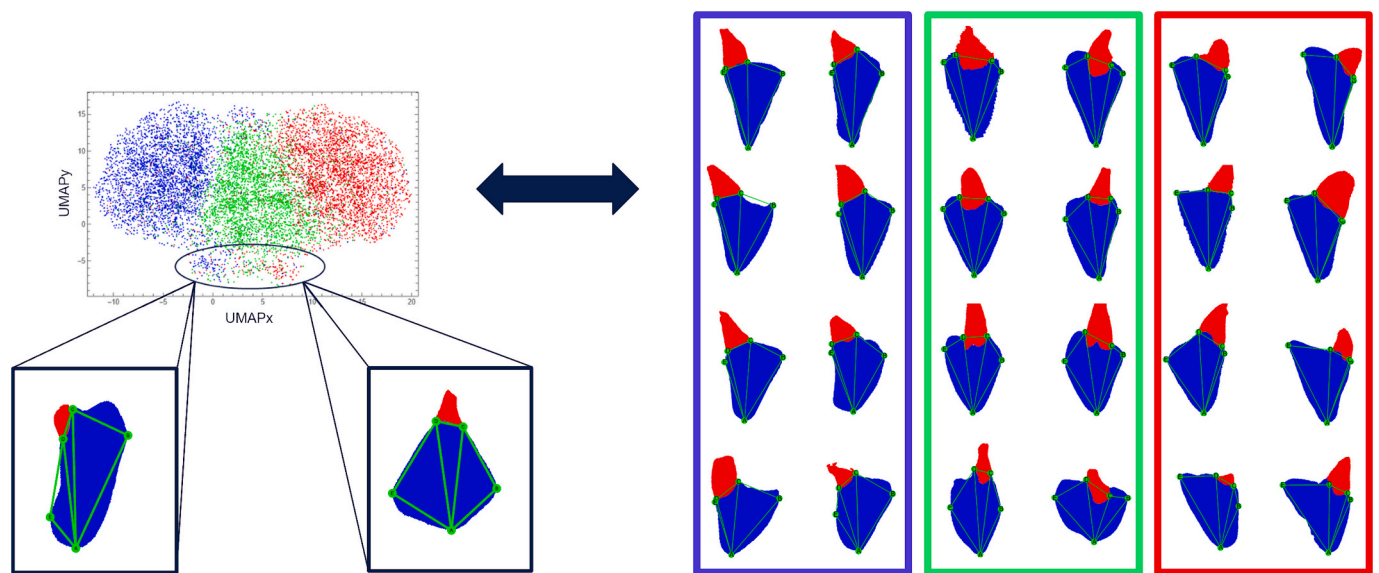


Fig. 7. Mapping of cardiac morphological variation in Atlantic salmon based on the Uniform Manifold Approximation and Projection (UMAP) dimension reduction of the heart measurements. Raw output images of the segmentation model, showing the probability of ventricle (blue) and bulbus (red) and the landmark points (A, B, C, D and E). Heart images are visualized in three different projections, including left lateral (blue points), ventrodorsal (green points), and right lateral (red points). Note the outliers (i.e., clusters at the center bottom of the UMAP), where heart images with extreme heart shape deformities have been circled and highlighted. (For interpretation of the references to colour in this figure legend, the reader is referred to the web version of this article.)

deviation (Engdal et al., 2024). Hence, a challenge with our morphometric method when applied to higher dimensional data, is the interpretability in relation to the human recognizable traits.

4.2. Heart shape quantification

Dimension reduction helps to find key features that distinguish the samples in a dataset, and we used it to identify key features distinguishing salmon heart shapes based on the measurement of 5 landmark points. We tried different approaches, including standard principal components analysis (PCA), t-distributed stochastic neighbor embedding (t-SNE) (Van Der Maaten and Hinton, 2008) and UMAP (McInnes et al., 2018). UMAP was chosen because it showed ability to separate images of different heart projections (horizontal axis in Fig. 5), indicating that it is able to detect some geometric characteristics. The other methods mentioned above were not able to clearly separate different projections which made it difficult to interpret the output.

The horizontal axis in Fig. 7 captures the symmetry of the heart images, which is related to the lengths of AB, AC and BC relative to AE, AD and DE, and correlates with the projection of the heart images. For left lateral projections, one expects that the left dorsal ventricular apex (B) will be further out from the heart center than the ventral ventricular apex (E), and opposite for RL projections. For VD projections, one expects the ventral ventricular apex (E) and left dorsal ventricular apex (B) to be at a similar distance from the center of the ventricle. The reason why the different heart projections cannot be perfectly separated may be due to both the variation in the angle images are taken from, and the fact that heart shape symmetry varies. For images of a particular projection, the variation along the horizontal axis gives an indication of how pronounced the ventral ventricular apex and the left dorsal ventricular apex are. When we look at the heart images along a vertical axis in Fig. 7, we see that it correlates with the lengths of AB, AC, AD and AE, meaning that the vertical axis relates to the ratio of the ventricle height and ventricle width. This suggests that the ventricular height:width ratio

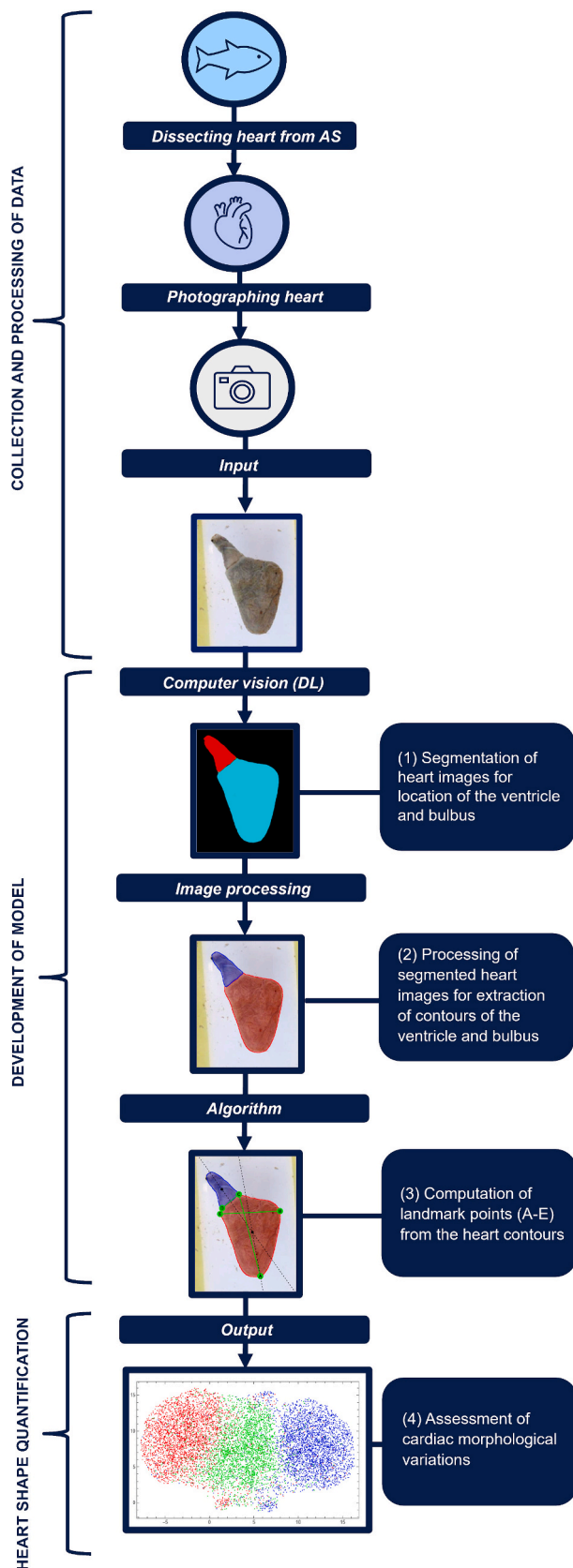


Fig. 8. The process flow from sampling of the Atlantic salmon (AS), followed by dissecting out and photographing its heart (visualized in left lateral projection), then using deep learning (DL) for the development of the image segmentation model, and lastly, applying an algorithm to enable an automated morphometric analysis of the Atlantic salmon heart.

used by previous research studies (Engdal et al., 2024; Frisk et al., 2020) is a useful geometric parameter, according to our morphometric method. We have done some preliminary analysis to correlate the UMAP heart shape quantification with other parameters. We see variation in distribution of the points for Norway versus the Faroe Islands (as shown in Fig. 6), however the differences could be due to how the photos were taken in Norway and the Faroe Islands. We also note that we have much more images from Norway, which could explain the larger variation in Norway.

Fig. S1 shows an example of how the statistical analysis of the UMAP output could potentially be used to compare heart shapes in different populations of Atlantic salmon. It is important to note here that such comparisons are only meaningful if the samples are representative of the underlying populations being compared. In the present study, our data originates from a limited number of producers, several unknown variables vary between the sites where hearts were harvested and there is large variation in sample size between the different categories (Table S1). Thus, it is not reasonable to assume that our samples are representative for the larger populations they represent, and statistical differences should be treated with care. This is especially true for the comparison between farmed populations of salmon, where the analysis indicate that hearts of farmed Atlantic salmon from the Faroe Islands had more elongated ventricular shape compared to the hearts of farmed Atlantic salmon from Norway (Fig. S1). With regards to comparison between farmed and wild fish, our analysis indicate that wild Atlantic salmon tend to have more elongated ventricular shapes compared to the farmed Atlantic salmon hearts. This finding is in line with previous research comparing heart shapes of wild and farmed salmonids (Poppe et al., 2003; Engdal et al., 2024). Our hope is that by supplementing our shape quantification data with other data, we may be able to detect meaningful correlations and explain the differences between environments or genetic backgrounds in future work.

The bottom cluster in Fig. 5 contains outliers, seemingly images with extreme cardiac morphological deviations and where the location of the landmark points A-E can be highly ambiguous. We generally see that the five landmark points A-E are insufficient for measuring extreme deviations, consistent with what Engdal et al. (2024) used. This suggests that complex morphometrics should entail more than just measuring the heart shape and looking at the different ways to quantify heart shape, that better capture the full geometry of the hearts. Better quantification of the heart shape could be achieved by quantifying the boundary shape of the heart (i.e., the full contour in accordance with the outline-based GM method) including the ventricle and bulbus, rather than only using the five landmark points presented in this study. Namely, an important limitation of such a landmark-based GM approach is that despite the number of landmark points used they may still not be sufficient to capture the shape of a structure, since shape differences could be located in the regions between the landmark points (Adams et al., 2004). However, the contour has shown promising results in previous research to accurately reflect the general shape and may also highlight traits that are not distinguishable by the naked eye (Lishchenko and Jones, 2021). Possible further investigations could be to train machine learning classifier on heart contours from both survivors and deceased fish and use explainability-techniques to determine which features are important for the classification. Another way to strengthen the assessment for revealing the true variation in morphological traits could also be to combine the qualitative and quantitative approaches as previously suggested by Engdal et al. (2024). Lastly, since our method only was developed on fixated hearts it needs to be validated for fresh or chilled hearts before it can be used in the field. Thus, in the future, morphological analysis may be utilized to document change in shape related to fixation in order to recommend the most effective methods for high-throughput imaging.

5. Conclusion

A key deliverable of this study has been the development of a deep learning model for computer vision and an algorithm to detect cardiac morphological deviations in farmed Atlantic salmon. Using the concept of a morphometric analysis, it was possible to quantify the shape of Atlantic salmon hearts by identifying landmark points on the hearts and calculating the distances between them. The morphometric scores obtained in this way were used to classify heart images. Our method was able to successfully differentiate between the three different projections (VD, LL and RL) at which the heart images were taken and identified ventricle elongation as a key distinguishing feature. As a result, we achieved a more objective cardiac morphological analysis that has the potential to inform approaches to improve fish welfare and sustainable growth in aquaculture in the long term.

Funding

This study was partially funded by NordForsk (grant number: 103385) in compliance with EU rules on state aid. NordForsk had no role in study design, data collection, analysis, or interpretation of data, in writing the manuscript or in the decision to submit the manuscript for publication.

CRedit authorship contribution statement

Lisa-Victoria Bernhardt: Writing – review & editing, Writing – original draft, Visualization, Project administration, Data curation, Conceptualization. **Andreas Hafver:** Writing – review & editing, Writing – original draft, Visualization, Validation, Software, Methodology, Investigation, Formal analysis, Data curation, Conceptualization. **Nafiha Usman:** Writing – review & editing, Visualization, Project administration, Data curation, Conceptualization. **Edward Yi Liu:** Writing – review & editing, Software, Formal analysis. **Jørgen Andreas Åm Vatn:** Writing – review & editing, Project administration, Funding acquisition, Conceptualization. **André Ødegårdstuen:** Writing – review & editing, Software, Methodology, Formal analysis. **Heidi S. Mortensen:** Writing – review & editing. **Ida Beitnes Johansen:** Writing – review & editing, Supervision, Resources, Project administration, Methodology, Funding acquisition, Conceptualization.

Declaration of competing interest

The authors declare that they have no known competing financial interests or personal relationships that could have appeared to influence the work reported in this paper.

Data availability

The authors do not have permission to share data.

Appendix A. Supplementary data

Supplementary data to this article can be found online at <https://doi.org/10.1016/j.aquaculture.2024.741145>.

References

- Adams, D.C., Rohlf, F.J., Slice, D.E., 2004. Geometric morphometrics: Ten years of progress following the 'revolution'. *Ital. J. Zool.* 71 (1), 5–16. <https://doi.org/10.1080/11250000409356545>.
- Claireaux, G., McKenzie, D.J., Genge, A.G., Chatelier, A., Aubin, J., Farrell, A.P., 2005. Linking swimming performance, cardiac pumping ability and cardiac anatomy in rainbow trout. *J. Exp. Biol.* 208 (10), 1775–1784. <https://doi.org/10.1242/jeb.01587>.
- Deng, J., Dong, W., Socher, R., Li, L.-J., Li, K., Fei-Fei, L., 2009. ImageNet: a large-scale hierarchical image database. *IEEE Conference on Computer Vision and Pattern Recognition 2009*, 248–255. <https://doi.org/10.1109/CVPR.2009.5206848>.
- Engdal, V.A., Dalum, A.S., Kryvi, H., Frisk, M., Torsvik, H., Hodne, K., Romstad, H., Johansen, I.B., 2024. State of the heart: anatomical annotation and assessment of morphological cardiac variation in Atlantic salmon (*Salmo salar* L.). *Aquaculture* 578. <https://doi.org/10.1016/j.aquaculture.2023.740046>.
- Frisk, M., Høyland, M., Zhang, L., Vindas, M.A., Øverli, Ø., Johansen, I.B., 2020. Intensive smolt production is associated with deviating cardiac morphology in Atlantic salmon (*Salmo salar* L.). *Aquaculture* 529, 735615. <https://doi.org/10.1016/J.AQUACULTURE.2020.735615>.
- Grefsrud, E.S., Agnalt, A.-L., Andersen, L.B., Diserud, O., Dunlop, K.M., Escobar, R., Fiske, P., Folkedal, O., Glover, K., Grøsvik, B.E., Halvorsen, K., Hannisdal, R., Hansen, P.K., Hindar, K., Husa, V., Jansson, E., Johnsen, I.A., Karlsen, Ø., Karlsson, S., ... Wennevik, V., (2024). Risk report Norwegian fish farming 2024 - Production mortality in farmed fish and environmental effects of Norwegian fish farming. Rapport fra havforskningen, number 4. <https://www.hi.no/hi/nettrapporter/rapport-fra-havforskningen-2024-4#sec-2-1>.
- He, K., Zhang, X., Ren, S., Sun, J., 2015. Spatial pyramid pooling in deep convolutional networks for visual recognition. *IEEE transactions on pattern analysis and machine intelligence* 37 (9), 1904–1916. <https://doi.org/10.1109/TPAMI.2015.2389824>.
- Lishchenko, F., Jones, J.B., 2021. Application of shape analyses to recording structures of marine organisms for stock discrimination and taxonomic purposes. In: *Frontiers in Marine Science*, vol. 8. Frontiers Media S.A. <https://doi.org/10.3389/fmars.2021.667183>
- Liu, H., Ma, X., Yu, Y., Wang, L., Hao, L., 2023. Application of deep learning-based object detection techniques in fish aquaculture: a review. *Journal of Marine Science and Engineering* 11 (4), 867.
- McInnes, L., Healy, J., Melville, J., 2018. UMAP: Uniform Manifold Approximation and Projection for Dimension Reduction. <http://arxiv.org/abs/1802.03426>.
- Oliveira, V.H.S., Dean, K.R., Qviller, L., Kirkeby, C., Bang Jensen, B., 2021. Factors associated with baseline mortality in Norwegian Atlantic salmon farming. *Sci. Rep.* 11 (1) <https://doi.org/10.1038/s41598-021-93874-6>.
- Poppe, T., Johansen, R., Gunnes, G., Tørud, B., 2003. Heart morphology in wild and farmed Atlantic salmon *Salmo salar* and rainbow trout *Oncorhynchus mykiss*. *Dis. Aquat. Org.* 57 (1–2), 103–108. <https://www.int-res.com/abstracts/dao/v57/n1-2/p103-108/>.
- Rohlf, J.F., Marcus, L.F., 1993. A revolution in Morphometrics. Reprinted from *Trends in Ecology and Evolution* 8 (4).
- Sommerset, I., Wiik-Nielsen, J., Moldal, T., Oliveira, V.H.S., Svendsen, J.C., Haukaas, A., og Brun E., 2024. Fiskehelse rapporten 2023, Veterinærinstituttets rapportserie nr. 8a/2024, utgitt av Veterinærinstituttet 2024.
- Taylor, R.S., Kube, P.D., Evans, B.S., Elliott, N.G., 2015. Genetic selection for amoebic gill disease (AGD) resilience in the Tasmanian Atlantic salmon (*Salmo salar*) breeding program. <https://www.frdc.com.au/sites/default/files/products/2011-77/1-DLD.pdf>.
- Van Der Maaten, L., Hinton, G., 2008. Visualizing Data using t-SNE. In: *J. Mach. Learn. Res.* 9.
- Waskom, M., 2021. seaborn: statistical data visualization. *J. Open Source Softw.* 6 (60), 3021. <https://doi.org/10.21105/joss.03021>.
- Wolfram Research, Inc, 2024. Mathematica, Version 14.0. Champaign, IL. <https://www.wolfram.com/mathematica>.
- Xie, S., Girshick, R., Dollár, P., Tu, Z., He, K., 2016. Aggregated residual transformations for deep neural networks. <http://arxiv.org/abs/1611.05431>.
- Zhao, S., Zhang, S., Liu, J., Wang, H., Zhu, J., Li, D., Zhao, R., 2021. Application of machine learning in intelligent fish aquaculture: a review. *Aquaculture* 540, 736724. <https://doi.org/10.3390/jmse11040867>.